Cite this: *Dalton Trans.*, 2018, **47**, 16596

A mononuclear five-coordinate Co(II) single molecule magnet with a spin crossover between the $S = 1/2$ and $3/2$ states†

Lei Chen,^a Jingbo Song,^a Wen Zhao,^a Gangji Yi,^a Zhikuan Zhou,^a ^a Aihua Yuan,^a ^{*a} You Song,^b ^{*b} Zhenxing Wang^c ^c and Zhong-Wen Ouyang^c

Although a great number of single-ion magnets (SIMs) and spin-crossover (SCO) compounds have been discovered, multifunctional materials with the combination of SCO and SIM properties are extremely scarce. Here magnetic studies have been carried out for a mononuclear, five-coordinate cobalt(II) complex [Co(3,4-lut)₄Br]Br (**1**) with square pyramidal geometry. Direct-current magnetic measurement confirms the spin transition between the $S = 1/2$ and $3/2$ states in the range of 150–290 K with a small hysteresis loop. Frequency- and temperature-dependent alternating-current magnetic susceptibility reveals slow magnetization relaxation under an applied dc field of 3000 Oe. The work here presents the first instance of the five-coordinate mononuclear cobalt(II)-based SIM exhibiting the thermally induced complete SCO.

Received 19th September 2018,
Accepted 23rd October 2018

DOI: 10.1039/c8dt03783c

rsc.li/dalton

Introduction

In recent years, enormous research efforts have been devoted to the construction of single molecule magnets (SMMs) based on mononuclear highly anisotropic paramagnetic f- and d-block ions, which are also known as single-ion magnets (SIMs).^{1,2} Recent breakthroughs have been observed in lanthanide-based SIMs, including the stable pentagonal bipyramidal Dy(III)-based SIMs with an ultra-high energy barrier and the dysprosium metallocene complex [(Cp^{ttt})₂Dy][B(C₆F₅)₄] with a record energy barrier of 1837 K and a blocking temperature of 60 K.^{3,4} For the 3d transition metal system, numerous SIMs based on the 3d ions containing Cr(I),⁵ Cr(II),⁶ Mn(II/III/IV),^{7–9} Fe(I/II/III),^{10–12} Ni(I/II/III),^{13,14} Cu(II)¹⁵ and Co(I/II)^{16,17} have coordination numbers ranging from two to eight in different coordination geometries.¹⁸ In this regard, the high-spin (HL) Co(II)-SIMs dominated the majority because their large magnetic anisotropy derived from the unquenched angular momentum and significant spin-orbit coupling.¹⁷

Further great attention in the field of molecular magnetism focused on spin-crossover (SCO) materials, owing to their potential application in binary switching, chemosensors, information storage and electronic devices.¹⁹ To date, most of the SCO complexes refer to Fe(II) and Fe(III) ions,²⁰ and to a lesser extent Co(II).^{17i,21–24} Due to the transition involving just one electron for the d⁷ Co(II) system, SCO for the Co(II) complexes is often incomplete, whereas few examples of Co(II) complexes exhibit the appearance of hysteresis associated with thermal transitions which is the common feature of Fe(II) systems. The majority of reported SCO Co(II)-based complexes so far involve mononuclear six-coordinate species^{21,22} and only a few cases of four- and five-coordinate complexes.^{17i,21,23,24}

Although many SIMs and SCO compounds have been reported, mononuclear Co(II) complexes showing both magnetic properties have not been documented in the literature except one example.¹⁷ⁱ Co(II)-based SIMs favour the large ground spin state ($S = 3/2$) to enhance the energy barrier (U_{eff}), whereas SCO complexes generally possess the low-spin (LS) states ($S = 1/2$) at low temperature. Therefore, it is not easy to observe the coexistence of SCO and SIM behaviors in the same mononuclear compound. In this paper, we report the structural characterization, electron paramagnetic resonance (EPR) and magnetic studies of complex [Co(3,4-lut)₄Br]Br (3,4-lut = 3,4-lutidine, **1**). This complex with an axisymmetric square pyramidal geometry simultaneously displays thermally induced spin transition and slow magnetic relaxation which is unexpected for the LS state ($S = 1/2$). This work represents the first square pyramidal Co(II)-based SIM that possesses a complete SCO.

^aSchool of Environmental and Chemical Engineering, Jiangsu University of Science and Technology, Zhenjiang 212003, P. R. China. E-mail: aihua.yuan@just.edu.cn

^bState Key Laboratory of Coordination Chemistry, Nanjing National Laboratory of Microstructures, School of Chemistry and Chemical Engineering, Nanjing University, Nanjing 210093, P. R. China. E-mail: yousong@nju.edu.cn

^cWuhan National High Magnetic Field Center & School of Physics, Huazhong University of Science and Technology, Wuhan 430074, P. R. China

† Electronic supplementary information (ESI) available: Experimental section including synthesis and physical measurements, detailed crystallographic data, XRD patterns, and magnetic data. CCDC 1866414 and 1866415. For ESI and crystallographic data in CIF or other electronic format see DOI: 10.1039/c8dt03783c

Experimental section

General considerations

All chemicals were obtained from commercial sources and used as received without further purification. All manipulations were performed by using standard Schlenk techniques under a nitrogen atmosphere. Elemental analyses for C, H and N were carried out on an Elementar Vario EL III elemental analyzer. The powder X-ray diffraction (PXRD) patterns for polycrystalline samples were collected at room temperature on a Bruker D8 Advance X-ray diffractometer.

Synthesis of [Co(3,4-lut)₄Br]Br (1)

Complex **1** was prepared according to a modified method in the literature.²⁵ The ligand 3,4-lutidine (10 mmol, 1.1 mL) was added to a solution of anhydrous CoBr₂ (1.0 mmol, 0.237 g) in 20.0 mL extra dry acetonitrile. The mixture was allowed to stand overnight at -10 °C, which gave dark green crystals in 41.2% yield based on the Co content. Elemental analysis (%) calcd for CoC₂₈H₃₆Br₂N₄ (MW 647.36): C, 51.95; H, 5.56; N, 8.66. Found: C, 51.89; H, 5.58; N, 8.70.

X-ray structure determination

Single crystal of **1** with appropriate dimensions was measured on a Bruker APEX II diffractometer at 298 K and 123 K equipped with a CCD area detector (Mo K α radiation, λ = 0.71073 Å).²⁶ The APEX II program was employed for data collection and determination of unit-cell parameters. The data were integrated and corrected by using SAINT. Absorption corrections were applied with SADABS.²⁷ The structures were solved by using SHELXS-97 and subsequently completed by Fourier recycling using the SHELXL 2014 program.²⁸ All non-hydrogen atoms were refined with anisotropic displacement parameters. Hydrogen atoms on organic ligands were set at the calculated positions and generated by using the riding model.

Magnetic measurements

Direct-current (dc) magnetic measurement of **1** was performed at fields up to 7 T between 1.8 and 300 K on a Quantum Design SQUID VSM magnetometer at 1 kOe. Alternating-current (ac) susceptibility measurement was carried out on a Quantum Design MPMS-XL17 SQUID instrument at ac frequencies ranging from 1 to 1500 Hz under different applied static fields with an oscillating ac field of 5 Oe. The magnetic susceptibility data were corrected for diamagnetism of the constituent atoms and sample holder estimated by using Pascal constants.

HF-EPR measurements were performed on a locally developed spectrometer at the National High Magnetic Field Laboratory, using a superconducting magnetic field of up to 17 T.²⁹

Results and discussion

Complex [Co(3,4-lut)₄Br]Br (**1**) was synthesized by the reaction of an excess amount of 3,4-lutidine in the presence of CoBr₂ in methanol to give dark green crystals. The structure data of **1**

have already been reported in 1996.²⁵ Here the crystal structure of **1** was re-determined by single-crystal X-ray diffraction analysis at 296 K and 123 K in order to investigate the possible temperature-induced structural changes. The unit cell and structure refinement data and the selected bond lengths and angles for **1** are listed in Table S1† and Table 1. Both **1**-296 K and **1**-123 K display the same monoclinic *C2/c* space group, suggesting no structural phase transition. Only three cell axes are slightly shorter for **1**-123 K than for **1**-296 K, so that a decrease in the cell volume (5.5%) occurs in this complex as the temperature changes from 296 to 123 K.

The coordination sphere of Co(II) is an axisymmetric square pyramidal geometry, in which four nitrogen atoms of four 3,4-lutidine molecules form the basal plane whereas one bromide ion locates at the apex (Fig. 1). As depicted in Table 1, the Co–N bond lengths are 2.110(4) and 2.136(4) Å at 296 K, which is longer than those (1.9686(18) and 1.9677(18) Å) at 123 K. These

Table 1 Selected bond lengths (Å) and angles (°) for **1**

	1-296 K	1-123 K
Bond lengths (Å)		
Co–N1	2.110(4)	1.9686(18)
Co–N2	2.136(4)	1.9677(18)
Co–Br1	2.5145(13)	2.6345(5)
Angles (°)		
N1–Co–N2	87.37(17)	88.16(7)
N1–Co–N2a	89.26(17)	90.36(7)
N1a–Co–N1	157.4(3)	165.40(10)
N2–Co–N2a	162.7(3)	168.36(10)
N1–Co–Br1	101.28(13)	97.30(5)
N2–Co–Br1	98.64(13)	95.82(5)

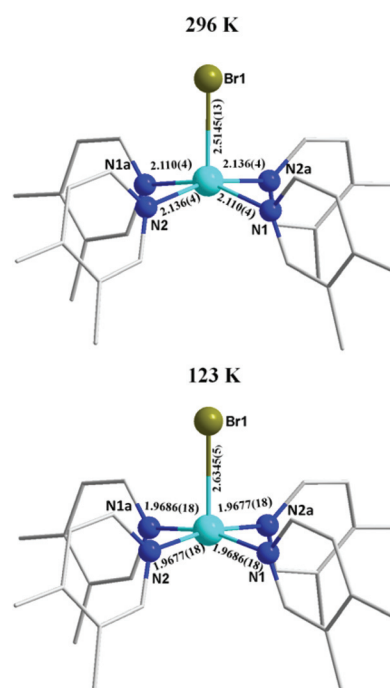


Fig. 1 Structures of the cation [Co(3,4-lut)₄Br]⁺ at 296 and 123 K.

Co–N bond lengths at different temperatures are respectively identical to the average standard bond lengths (Co–N = 2.12 (HL) and 1.94 (LS)) for the reported five-coordinate complexes, which implies the possibility of thermally induced spin-crossover.^{24b} The apical Co–Br bond increases from 2.5145(13) to 2.6345(5) Å with cooling temperature, exceeding that of the reported five-coordinate Co(II) complexes.^{24b–d,30} A small increase of the N–Co–N angles in the basal plane accompanied by the marked reduction of the apical Br–Co–N angles were observed on going from 296 to 123 K. The Co(II) ion deviates from the basal N₄ plane by 0.3670 Å at 296 K and 0.2248 Å at 123 K. These structural changes confirm that an increasing elongated axial distortion of the square pyramidal structure occurred at 123 K, which could be favourable for the LS state.^{24b} Continuous shape measurement analyses using the SHAPE program afford the values of 0.281 at 296 K and 0.784 at 123 K relative to the square pyramid (Table S2†),³¹ indicating the higher distortion at 123 K than at 296 K. The shortest distances between the pyridine ring centroids of 5.104 Å at 296 K and 5.090 Å at 123 K suggest the non-existence of π – π stacking interactions (Fig. S1 and S2†). The nearest intermolecular Co–Co distances are 8.394 Å at 296 K and 8.364 Å at 123 K (Fig. S3 and S4†), respectively, thus hindering the intermolecular exchange interactions.

The phase purity of the bulk sample of **1** used for the magnetic measurements was confirmed by PXRD spectra (Fig. S5†). To elucidate the magnetic properties, SQUID magnetometer measurements were carried out for a polycrystalline sample of **1**. Variable-temperature direct-current (dc) magnetic susceptibility was investigated under a field of 1000 Oe in the temperature range of 1.8–310 K. As shown in Fig. 2, the $\chi_M T$ value for **1** is equal to 2.92 cm³ K mol^{−1} at 310 K, corresponding to an isolated HS Co(II) ion with $g = 2.50$. When the temperature is decreased from 290 K, the $\chi_M T$ value rapidly drops, reaching 0.47 cm³ K mol^{−1} at 1.8 K, which is in the range of values expected for a LS Co(II) center. The spin transition from the LS to the HS state with a small hysteresis loop occurs in the range of 150–290 K. We note that there is a rare case of the square pyramidal mononuclear cobalt(II) complex with the spin-crossover. The fit of magnetic susceptibility from 1.8 to 130 K yields $g_{\text{iso}} = 2.23$,³² which is larger than the spin-only value of 2.0032, indicating the presence of spin-orbit coupling and an anisotropic ground doublet in **1**. EPR spectra of a microcrystalline powder sample of **1** at 4 K with a frequency of 302.4 GHz, shown in Fig. 2, are satisfactorily simulated as an $S = 1/2$ spin system, yielding the g -factors of $g_1 = 2.3986(5)$, $g_2 = 2.3857(5)$, and $g_3 = 2.0063(5)$. The average g value ($g_{\text{av}} = [(g_1 + g_2 + g_3)/3] = 2.26$) is in accord with the g_{iso} value (2.23) determined from fitting the magnetic susceptibility.

The magnetization dynamics behavior of **1** was investigated by measurements of alternative-current magnetic susceptibility at 1.8 K under different external dc fields from 0 to 4000 Oe (Fig. S6†). Under zero static magnetic field, the out-of-phase (χ''_M) components exhibit no frequency dependence. However, upon application of an external dc field, the frequency-depen-

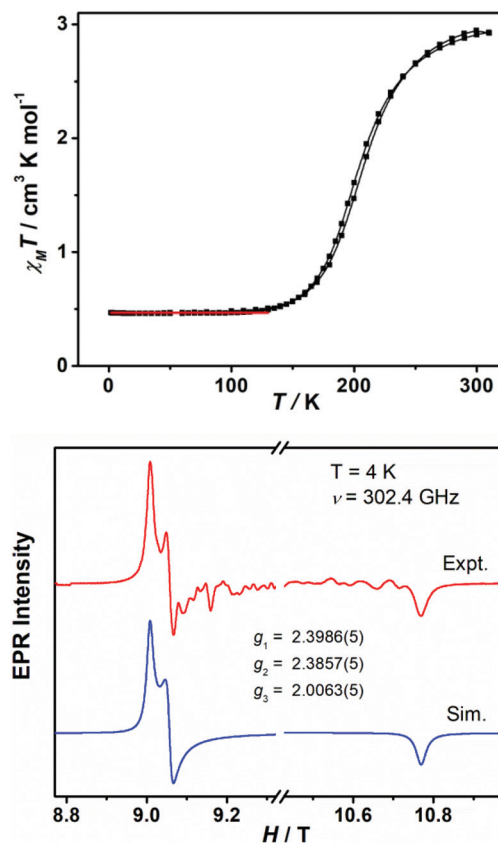


Fig. 2 Variable-temperature dc susceptibility data of **1** under an applied dc field of 0.1 T. The red line represents the fit with the PHI program (top).³² EPR spectra for **1** at 4 K with the frequency of 302.4 GHz (bottom).

dent χ''_M maximum peaks appear in the applied frequencies. With the increase of the external dc field, these maxima intensify but their positions remain almost the same (the range of 3.0–5.0 Hz). Upon further increasing the dc field, the intensity of the χ''_M peaks slightly reduces starting at 3500 Oe. Therefore, variable-frequency ac magnetic susceptibilities at different temperatures were investigated under an optimum field of 3000 Oe (Fig. 3 and S7†). The χ''_M magnetic susceptibility exhibits strong frequency- and temperature-dependence, indicating the presence of slow dynamics of magnetization in **1**.

As depicted in Fig. 3, the frequency dependent χ''_M peaks were observed at the temperatures from 1.8 to 14 K. Thus, at whole temperatures, the Cole–Cole data were modelled by using a generalized Debye function (Fig. S8 and Table S3†),³³ in order to extract the relaxation time τ . The α values within the range of 0.03–0.49 suggest multiple relaxation processes. It is a conventional operation that the temperature dependence relaxation time τ was fitted with an Arrhenius law $\tau = \tau_0 \exp(U_{\text{eff}}/k_B T)$ based on the assumption of a thermally activated (Orbach) process, which gives an energy gap of 40.9 K with a pre-exponential factor $\tau_0 = 8.3 \times 10^{-6}$ s (Fig. S9†). The large value of τ_0 is far beyond expected for typical vibrations of the

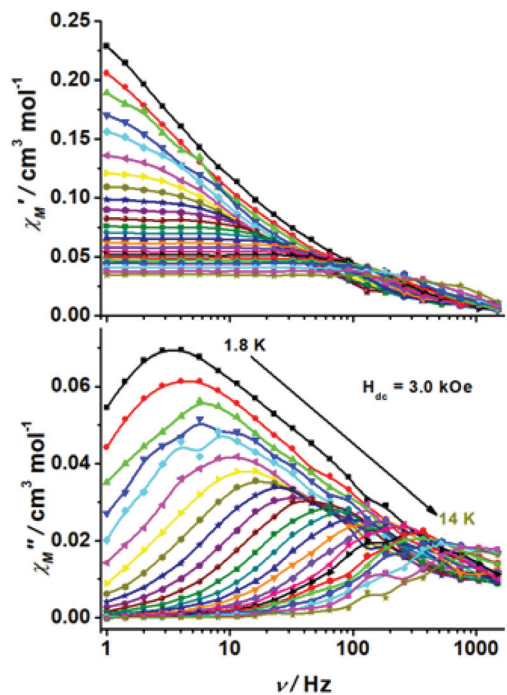


Fig. 3 Frequency-dependence of the in-phase and out-of-phase susceptibility between 1.8 and 14 K under a 3.0 kOe applied dc field.

network which govern the Orbach reversal of magnetization, in line with the lack of electronic states that can be thermally populated providing a path for the multiphonon Orbach mechanism of relaxation.³⁴ Thus, the plot of $\ln(\tau)$ vs. T^{-1} can be reproduced by the combination of the QTM, direct and Raman mechanisms:

$$\tau^{-1} = \frac{B_1}{1 + B_2 H^2} + A H^4 T + b T^n \quad (1)$$

To avoid overparameterization, the field-dependent τ values extracted from the peaks of frequency dependent χ''_M (Fig. S6†) were modelled by the inclusion of the QTM and direct terms, given that the quantum tunneling of magnetization (QTM) and direct processes are field-dependent. A successful fit was obtained, as depicted in Fig. S10.† Then $B_1 = 29.69 \text{ s}^{-1}$, $B_2 = 0.044 \text{ kOe}^{-2}$ and $A = 0.014 \text{ s}^{-1} \text{ kOe}^{-4}$ were used in modelling the $\ln(\tau)$ vs. T^{-1} data using eqn (1). Fig. 4 shows that the fit is in accord with the experimental data of the temperature dependent relaxation time τ over the whole temperature, with the Raman parameters of $b = 0.55 \text{ s}^{-1} \text{ K}^{-n}$ and $n = 3.5$. For the Kramers ions, the exponent $n = 9$ should be expected for the Raman process. Nevertheless, in this case the exponent value of $n = 3.5$ implies a Raman-like process involving both acoustic (lattice) and optical (molecular) vibrations, which is observed for many 3d-ion SIMs. Furthermore, these parameter values were employed to construct the individual contributions of the QTM, direct and Raman processes in the whole temperature range (Fig. 4). It can be seen that the region of 2.7–14 K is dominated by the Raman-like process while the contributions

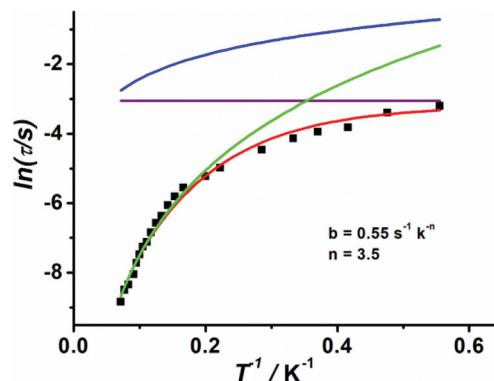


Fig. 4 Temperature dependence of the magnetization relaxation rates under a 3.0 kOe applied dc field. The red line represents the best fit by using eqn (1). The other lines represent data fits using the QTM (purple), direct (blue) and Raman processes (green).

of the QTM process are dominating in the temperature range of 1.8–2.7 K.

It is well known that SMM behavior results from the reversal of spin overcoming an energy barrier, which is governed by a ground spin state larger than $S = 1/2$ accompanied by a negative axial zero-field splitting. However, it is incredible that several cases of the $S = 1/2$ systems involving mononuclear $V(\text{IV})$,^{34a,35} $Mn(\text{IV})$,⁹ $Co(\text{II})$,¹⁷ⁱ $Ni(\text{I})$,¹³ $Ni(\text{III})$ ^{14c} and $Cu(\text{II})$ complexes exhibit slow magnetic relaxation behavior. Indeed, for the $S = 1/2$ systems, the spin-orbit coupling plays a crucial role in stabilizing an anisotropic ground doublet, resulting in the SMM behavior, except for the slow relaxation in the two coordinate mononuclear $Ni(\text{I})$ originating from the magnetic anisotropy with the unquenched orbital contribution. In the case of **1**, the dc magnetic data and EPR spectra confirm the significant anisotropy of the g tensor exceeding the spin-only value of 2.00232 and the spin-orbit coupling presented in the LS state of **1**. Thus, the detailed analysis of temperature dependence of the relaxation time suggests that this relaxation process can clearly be assigned to the combination of QTM and Raman mechanisms, rather than an Orbach process.

It is reported that the donor atoms and the axial elongation in square pyramidal complexes play an important role in determining whether the metal atom is in a high- or low-spin state.^{24b,30} On the one hand, it has been found that the soft donor atoms afford a high field strength, thus resulting in the LS state, whilst the hard atoms with a low field strength are favoured for the HS complexes.^{24,30} The chloride (soft) and iodide (hard) atoms are found in high- and low-spin complexes, whereas the donor atom bromide is very likely to lead to spin-crossover properties.²⁴ On the other hand, in square pyramidal geometry, lengthening of the axial bond with simultaneous shortening of four basal bonds provides a square planar ligand field. In general, the square-planar $Co(\text{II})$ complexes are low spin, whereas the square pyramidal complex may be high spin. The temperature-dependent variation of the apical bond length in a square pyramidal five-coordinate

complex effects the spin multiplicity.^{24b} As a result, in the case of **1**, selecting Br as the apex coordinate atom has a decisive effect on the occurrence of SCO. As previously mentioned for the structural analysis of **1**, when the temperature changed from 296 K to 123 K, the length of the Co–Br apical bond increased while shortening of the four Co–N basal bonds was observed, which is a typical characteristic of a SCO system with square pyramidal geometry.

Conclusions

In summary, we have reported here the temperature-dependent structure and magnetic properties of the mononuclear complex [Co(3,4-lut)₄Br]Br (**1**). The X-ray structure analysis indicates the higher elongated axial distortion of the square pyramidal configuration around the Co(II) centre at 123 K, compared to the structure at 296 K. The magnetization study confirms that both the abrupt SCO with a small hysteresis loop and slow magnetic relaxation behaviors were simultaneously observed in **1**. Interestingly, the slow relaxation arises from the low-spin state ($S = 1/2$) of Co(II) with the spin-orbit coupling. This work provides a new avenue to construct multifunctional molecular materials. Future effort along this line will focus on the current material displaying the abrupt hysteretic SCO as well as the SMM behavior.

Conflicts of interest

There are no conflicts to declare.

Acknowledgements

This work was supported by the National Natural Science Foundation (21601070, 51672114, 21701046, and 21501073), the China Postdoctoral Science Foundation (2016M601751), the Jiangsu Planned Projects for Postdoctoral Research Funds (1601037B), and the Natural Science Foundation of the Higher Education Institutions of Jiangsu Province (16KJB150012). A portion of this work was performed at the National High Magnetic Field Laboratory, which is supported by National Science Foundation Cooperative Agreement No. DMR-1157490 and the State of Florida.

Notes and references

- (a) G. A. Craig and M. Murrie, *Chem. Soc. Rev.*, 2015, **44**, 2135; (b) A. K. Bar, C. Pichon and J.-P. Sutter, *Coord. Chem. Rev.*, 2016, **308**, 346; (c) J. M. Frost, K. L. M. Harriman and M. Murugesu, *Chem. Sci.*, 2016, **7**, 2470; (d) L. Chen, J. J. Zhou, A. H. Yuan and Y. Song, *Dalton Trans.*, 2017, **46**, 15812.
- (a) D. N. Woodruff, R. E. P. Winpenny and R. A. Layfield, *Chem. Rev.*, 2013, **113**, 5110; (b) P. Zhang, Y.-N. Guo and J.-K. Tang, *Coord. Chem. Rev.*, 2013, **257**, 1728; (c) S. G. McAdams, A.-M. Ariciu, A. K. Kostopoulos, J. P. S. Walsh and F. Tuna, *Coord. Chem. Rev.*, 2017, **346**, 216.
- (a) Y.-C. Chen, J.-L. Liu, L. Ungur, J. Liu, Q.-W. Li, L.-F. Wang, Z.-P. Ni, L. F. Chibotaru, X.-M. Chen and M.-L. Tong, *J. Am. Chem. Soc.*, 2016, **138**, 2829; (b) J. Liu, Y.-C. Chen, J.-L. Liu, V. Vieru, L. Ungur, J.-H. Jia, L. F. Chibotaru, Y. Lan, W. Wernsdorfer, S. Gao, X.-M. Chen and M.-L. Tong, *J. Am. Chem. Soc.*, 2016, **138**, 5441; (c) Y.-S. Ding, N. F. Chilton, R. E. P. Winpenny and Y.-Z. Zheng, *Angew. Chem., Int. Ed.*, 2016, **55**, 16071.
- (a) C. A. P. Goodwin, F. Ortu, D. Reta, N. F. Chilton and D. P. Mills, *Nature*, 2017, **548**, 439; (b) F.-S. Guo, B. M. Day, Y.-C. Chen, M.-L. Tong, A. Mansikkamäki and R. A. Layfield, *Angew. Chem., Int. Ed.*, 2017, **56**, 11445.
- P. P. Samuel, R. Neufeld, K. C. Mondal, H. W. Roesky, R. Herbst-Irmer, D. Stalke, S. Demeshko, F. Meyer, V. C. Rojisha, S. De, P. Parameswaran, A. C. Stückl, W. Kaim, J. H. Christian, J. K. Bindra and N. S. Dalal, *Chem. Sci.*, 2015, **6**, 3148.
- (a) A. Cornia, L. Rigamonti, S. Boccedi, R. Clérac, M. Rouzières and L. Sorace, *Chem. Commun.*, 2014, **50**, 15191; (b) Y.-F. Deng, T. Han, Z. Wang, Z. Ouyang, B. Yin, Z. Zheng, J. Krzystek and Y.-Z. Zheng, *Chem. Commun.*, 2015, **51**, 17688; (c) J. H. Christian, D. W. Brogden, J. K. Bindra, J. S. Kinyon, J. van Tol, J. Wang, J. F. Berry and N. S. Dalal, *Inorg. Chem.*, 2016, **55**, 6376.
- A. C. Benniston, S. Melnic, C. Turta, A. B. Arauzo, J. Bartolomé, E. Bartolomé, R. W. Harrington and M. R. Probert, *Dalton Trans.*, 2014, **43**, 13349.
- (a) R. Ishikawa, R. Miyamoto, H. Nojiri, B. K. Breedlove and M. Yamashita, *Inorg. Chem.*, 2013, **52**, 8300; (b) A. Grigoropoulos, M. Pissas, P. Papatolis, V. Psycharis, P. Kyritsis and Y. Sanakis, *Inorg. Chem.*, 2013, **52**, 12869; (c) J. Vallejo, A. Pascual-Álvarez, J. Cano, I. Castro, M. Julve, F. Lloret, J. Krzystek, G. De Munno, D. Armentano, W. Wernsdorfer, R. Ruiz-García and E. Pardo, *Angew. Chem., Int. Ed.*, 2013, **52**, 14075; L. Chen, J. Wang, Y.-Z. Liu, Y. Song, X.-T. Chen, Y.-Q. Zhang and Z.-L. Xue, *Eur. J. Inorg. Chem.*, 2015, **2015**, 271; (d) A. Pascual-Álvarez, J. Vallejo, E. Pardo, M. Julve, F. Lloret, J. Krzystek, D. Armentano, W. Wernsdorfer and J. Cano, *Chem. – Eur. J.*, 2015, **21**, 17299.
- M. Ding, G. E. Cutsail III, D. Aravena, M. Amoza, M. Rouzères, P. Dechambenoit, Y. Losovyj, M. Pink, E. Ruiz, R. Clérac and J. M. Smith, *Chem. Sci.*, 2016, **7**, 6132.
- (a) J. M. Zadrozny, D. J. Xiao, M. Atanasov, G. J. Long, F. Grandjean, F. Neese and J. R. Long, *Nat. Chem.*, 2013, **5**, 577; (b) P. P. Samuel, K. C. Mondal, N. A. Sk, H. W. Roesky, E. Carl, R. Neufeld, D. Stalke, S. Demeshko, F. Meyer, L. Ungur, L. F. Chibotaru, J. Christian, V. Ramachandran and J. van Tol, *J. Am. Chem. Soc.*, 2014, **136**, 11964; (c) C. G. Werncke, P. C. Bunting, C. Duhayon, J. R. Long, S. Bontemps and S. Sabo-Etienne, *Angew. Chem., Int. Ed.*, 2015, **54**, 245.

- 11 (a) J. M. Zadrozny, M. Atanasov, A. M. Bryan, C.-Y. Lin, B. D. Rekker, P. P. Power, F. Neese and J. R. Long, *Chem. Sci.*, 2013, **4**, 125; (b) A. A. Danopoulos, P. Braunstein, K. Y. Monakhov, J. van Leusen, P. Kögerler, M. Clémancey, J.-M. Latour, A. Benayad, M. Tromp, E. Rezabal and G. Frison, *Dalton Trans.*, 2017, **46**, 1163; (c) P.-H. Lin, N. C. Smythe, S. I. Gorelsky, S. Maguire, N. J. Henson, I. Korobkov, B. L. Scott, J. C. Gordon, R. T. Baker and M. Murugesu, *J. Am. Chem. Soc.*, 2011, **133**, 15806; (d) X. Feng, C. Mathonière, I.-R. Jeon, M. Rouzières, A. Ozarowski, M. L. Aubrey, M. I. Gonzalez, R. Clérac and J. R. Long, *J. Am. Chem. Soc.*, 2013, **135**, 15880; (e) A. Urtizberea and O. Roubeau, *Chem. Sci.*, 2017, **8**, 2290; (f) J. Xiang, J.-J. Liu, X.-X. Chen, L.-H. Jia, F. Yu, B.-W. Wang, S. Gao and T.-C. Lau, *Chem. Commun.*, 2017, **53**, 1474.
- 12 (a) S. Mossin, B. L. Tran, D. Adhikari, M. Pink, F. W. Heinemann, J. Sutter, R. K. Szilagyi, K. Meyer and D. J. Mindiola, *J. Am. Chem. Soc.*, 2012, **134**, 13651; (b) R. Sato, K. Suzuki, T. Minato, M. Shinoue, K. Yamaguchi and N. Mizuno, *Chem. Commun.*, 2015, **51**, 4081; (c) X. Feng, S. J. Hwang, J.-L. Liu, Y.-C. Chen, M.-L. Tong and D. G. Nocera, *J. Am. Chem. Soc.*, 2017, **139**, 16474; (d) T. Minato, D. Aravena, E. Ruiz, K. Yamaguchi, N. Mizuno and K. Suzuki, *Inorg. Chem.*, 2018, **57**, 6957.
- 13 (a) R. C. Poulten, M. J. Page, A. G. Algarra, J. J. Le Roy, I. López, E. Carter, A. Llobet, S. A. Macgregor, M. F. Mahon, D. M. Murphy, M. Murugesu and M. K. Whittlesey, *J. Am. Chem. Soc.*, 2013, **135**, 13640; (b) W. Lin, T. Bodenstern, V. Mereacre, K. Fink and A. Eichhöfer, *Inorg. Chem.*, 2016, **55**, 2091.
- 14 (a) K. E. R. Marriott, L. Bhaskaran, C. Wilson, M. Medarde, S. T. Ochsenbein, S. Hill and M. Murrie, *Chem. Sci.*, 2015, **6**, 6823; (b) G. A. Craig, A. Sarkar, C. H. Woodall, M. A. Hay, K. E. R. Marriott, K. V. Kamenev, S. A. Moggach, E. K. Brechin, S. Parsons, G. Rajaraman and M. Murrie, *Chem. Sci.*, 2018, **9**, 1551; (c) I. Bhowmick, A. J. Roehl, J. R. Neilson, A. K. Rappé and M. P. Shores, *Chem. Sci.*, 2018, **9**, 6564.
- 15 R. Boča, C. Rajnák, J. Titiš and D. Valigura, *Inorg. Chem.*, 2017, **56**, 1478.
- 16 Y.-S. Meng, Z. Mo, B.-W. Wang, Y.-Q. Zhang, L. Deng and S. Gao, *Chem. Sci.*, 2015, **6**, 7156.
- 17 (a) X.-N. Yao, J.-Z. Du, Y.-Q. Zhang, X.-B. Leng, M.-W. Yang, S.-D. Jiang, Z.-X. Wang, Z.-W. Ouyang, L. Deng, B.-W. Wang and S. Gao, *J. Am. Chem. Soc.*, 2017, **139**, 373; (b) Y.-F. Deng, Z. Wang, Z.-W. Ouyang, B. Yin, Z. Zheng and Y.-Z. Zheng, *Chem. – Eur. J.*, 2016, **22**, 14821; (c) J. M. Zadrozny and J. R. Long, *J. Am. Chem. Soc.*, 2011, **133**, 20732; (d) T. Jurca, A. Farghal, P.-H. Lin, I. Korobkov, M. Murugesu and D. S. Richeson, *J. Am. Chem. Soc.*, 2011, **133**, 15814; (e) J. Vallejo, I. Castro, R. Ruiz-García, J. Cano, M. Julve, F. Lloret, G. De Munno, W. Wernsdorfer and E. Pardo, *J. Am. Chem. Soc.*, 2012, **134**, 15704; (f) Y.-Y. Zhu, C. Cui, Y.-Q. Zhang, J.-H. Jia, X. Guo, C. Gao, K. Qian, S.-D. Jiang, B.-W. Wang, Z.-M. Wang and S. Gao, *Chem. Sci.*, 2013, **4**, 1802; (g) L. Chen, J. Zhou, H.-H. Cui, A.-H. Yuan, Z. Wang, Y.-Q. Zhang, Z.-W. Ouyang and Y. Song, *Dalton Trans.*, 2018, **47**, 2506–2510; (h) J. Zhou, J. Song, A. Yuan, Z. Wang, L. Chen and Z.-W. Ouyang, *Inorg. Chim. Acta*, 2018, **479**, 113; (i) H.-H. Cui, J. Wang, X.-T. Chen and Z.-L. Xue, *Chem. Commun.*, 2017, **53**, 9304; (j) L. Chen, S.-Y. Chen, Y.-C. Sun, Y.-M. Guo, L. Yu, X.-T. Chen, Z. Wang, Z.-W. Ouyang, Y. Song and Z.-L. Xue, *Dalton Trans.*, 2015, **44**, 11482; (k) L. Chen, J. Wang, J.-M. Wei, W. Wernsdorfer, X.-T. Chen, Y.-Q. Zhang, Y. Song and Z.-L. Xue, *J. Am. Chem. Soc.*, 2014, **136**, 12213.
- 18 (a) G. A. Craig and M. Murrie, *Chem. Soc. Rev.*, 2015, **44**, 2135; (b) A. K. Bar, C. Pichon and J.-P. Sutter, *Coord. Chem. Rev.*, 2016, **308**, 346; (c) J. M. Frost, K. L. M. Harriman and M. Murugesu, *Chem. Sci.*, 2016, **7**, 2470; (d) Y.-S. Meng, S.-D. Jiang, B.-W. Wang and S. Gao, *Acc. Chem. Res.*, 2016, **49**, 2381; (e) M. Feng and M.-L. Tong, *Chem. – Eur. J.*, 2018, **24**, 7574.
- 19 (a) O. Kahn and C. J. Martinez, *Science*, 1998, **279**, 44; (b) O. Sato, *Acc. Chem. Res.*, 2003, **36**, 692; (c) C. Atmani, F. El Hajj, S. Benmansour, M. Marchivie, S. Triki, F. Conan, V. Patinec, H. Handel, G. Dupouy and C. J. Gómez-García, *Coord. Chem. Rev.*, 2010, **254**, 1559; (d) M. A. Halcrow, *Spin-Crossover Materials: Properties and Applications*, Wiley, 2013.
- 20 (a) P. Gutlich, Y. Garcia and H. A. Goodwin, *Chem. Soc. Rev.*, 2000, **29**, 419; (b) M. Nihei, T. Shiga, Y. Maeda and H. Oshio, *Coord. Chem. Rev.*, 2007, **251**, 2606.
- 21 (a) H. A. Goodwin, *Top. Curr. Chem.*, 2004, **234**, 23; (b) I. Krivokapic, M. Zerara, M. L. Dakua, A. Vargas, C. Enachescu, C. Ambrusc, P. Tregenna-Piggott, N. Amstutz, E. Krausz and A. Hauser, *Coord. Chem. Rev.*, 2007, **251**, 364; (c) S. Hayami, Y. Komatsu, T. Shimizu, H. Kamihata and Y. H. Lee, *Coord. Chem. Rev.*, 2011, **255**, 1981; (d) R. G. Miller, S. Narayanaswamy, J. L. Tallon and S. Brooker, *New J. Chem.*, 2014, **38**, 1932.
- 22 (a) M. G. Cowan, J. Olguín, S. Narayanaswamy, J. L. Tallon and S. Brooker, *J. Am. Chem. Soc.*, 2012, **134**, 2892; (b) J. Palion-Gazda, B. Machura, R. Kruszynski, T. Granca, N. Moliner, F. Lloret and M. Julve, *Inorg. Chem.*, 2017, **56**, 6281–6296.
- 23 (a) D. M. Jenkins and J. C. Peters, *J. Am. Chem. Soc.*, 2003, **125**, 11162; (b) D. M. Jenkins and J. C. Peters, *J. Am. Chem. Soc.*, 2005, **127**, 7148.
- 24 (a) D. W. Shaffer, I. Bhowmick, A. L. Rheingold, C. Tsay, B. N. Livesay, M. P. Shores and J. Y. Yang, *Dalton Trans.*, 2016, **45**, 17910; (b) L. Sacconi, *Coord. Chem. Rev.*, 1972, **8**, 351; (c) W. S. J. Kelly, G. H. Ford and S. M. Nelson, *J. Chem. Soc. A*, 1971, 388; (d) W. V. Dahlhoff and S. M. Nelson, *J. Chem. Soc. A*, 1971, 2184.
- 25 J. Kansikas, M. Leskelä, G. Kenessey, T. Wadsten and G. Liptay, *Acta Chem. Scand.*, 1996, **50**, 267.
- 26 SMART & SAINT, *Software Reference Manuals, version 6.45*, Bruker Analytical X-ray Systems, Inc., Madison, WI, 2003.
- 27 G. M. Sheldrick, *SADABS – Software for Empirical Absorption Correction, version 2.05*, University of Göttingen, Göttingen, Germany, 2002.

- 28 (a) G. M. Sheldrick, *SHELXL97 – Program for Crystal Structure Refinement*, University of Göttingen, Göttingen, Germany, 1997; (b) G. M. Sheldrick, *Acta Crystallogr., Sect. C: Struct. Chem.*, 2015, **71**, 3–8.
- 29 (a) B. Cage, A. Hassan, L. Pardi, J. Krzystek, L. C. Brunel and N. S. Dalal, *J. Magn. Reson.*, 1997, **124**, 495; (b) A. Hassan, L. Pardi, J. Krzystek, A. Sienkiewicz, P. Goy, M. Rohrer and L. C. Brunel, *J. Magn. Reson.*, 2000, **142**, 300.
- 30 L. Sacconi, *J. Chem. Soc. A*, 1970, 248.
- 31 (a) S. Alvarez, P. Alemany, D. Casanova, J. Cirera, M. Llunell and D. Avnir, *Coord. Chem. Rev.*, 2005, **249**, 1693; (b) S. Alvarez and M. Llunell, *J. Chem. Soc., Dalton Trans.*, 2000, 3288.
- 32 N. F. Chilton, R. P. Anderson, L. D. Turner, A. Soncini and K. S. Murray, *J. Comput. Chem.*, 2013, **34**, 1164.
- 33 (a) K. S. Cole and R. H. Cole, *J. Chem. Phys.*, 1941, **9**, 341; (b) S. M. J. Aubin, Z. M. Sun, L. Pardi, J. Krzystek, K. Foltling, L. C. Brunel, A. L. Rheingold, G. Christou and D. N. Hendrickson, *Inorg. Chem.*, 1999, **38**, 5329.
- 34 (a) L. Tesi, E. Lucaccini, I. Cimatti, M. Perfetti, M. Mannini, M. Atzori, E. Morra, M. Chiesa, A. Caneschi, L. Sorace and R. Sessoli, *Chem. Sci.*, 2016, **7**, 2074; (b) K. N. Shrivastava, *Phys. Status Solidi B*, 1983, **117**, 437.
- 35 M. Atzori, E. Morra, L. Tesi, A. Albino, M. Chiesa, L. Sorace and R. Sessoli, *J. Am. Chem. Soc.*, 2016, **138**, 11234.